

UC Davis

UC Davis Previously Published Works

Title

Echocardiographic assessment of right ventricular systolic function in conscious healthy dogs following a single dose of pimobendan versus atenolol

Permalink

<https://escholarship.org/uc/item/4nr8d1gc>

Journal

Journal of Veterinary Cardiology, 17(3)

ISSN

1760-2734

Authors

Visser, Lance C
Scansen, Brian A
Brown, Nicole V
et al.

Publication Date

2015-09-01

DOI

10.1016/j.jvc.2015.04.001

Peer reviewed



ELSEVIER



Echocardiographic assessment of right ventricular systolic function in conscious healthy dogs following a single dose of pimobendan versus atenolol

Lance C. Visser, DVM, MS^{a,1}, Brian A. Scansen, DVM, MS^{a,*},
Nicole V. Brown, MS^b, Karsten E. Schober, DVM, PhD^a,
John D. Bonagura, DVM, MS^a

^a Department of Veterinary Clinical Sciences, College of Veterinary Medicine, The Ohio State University, 601 Vernon Tharp Street, Columbus, OH 43210, USA

^b Department of Biomedical Informatics, The Ohio State University, 2012 Kenny Road, Columbus, OH 43221, USA

Received 31 July 2014; received in revised form 1 April 2015; accepted 13 April 2015

KEYWORDS

Canine;
Cardiac;
Echocardiography;
Ultrasound

Abstract Objective: To quantify drug-induced changes in right ventricular (RV) systolic function after administration of pimobendan and atenolol.

Animals: 80 healthy privately-owned dogs.

Methods: Using a prospective, blinded, fully-crossed study design with randomized drug administration, RV systolic function was determined twice at two time periods; before and 3 h after administration of pimobendan (0.25 mg/kg PO) or atenolol (1 mg/kg PO). Indices of RV systolic function included tricuspid annular plane systolic excursion (TAPSE), fractional area change (FAC), pulsed-wave tissue Doppler-derived systolic myocardial velocity of the lateral tricuspid annulus (S'), and speckle-tracking-derived global longitudinal RV free wall strain and strain rate. The effect of treatment on percent change from baseline RV function was analyzed with a linear mixed model including the covariates heart rate, body weight, age, gender, drug sequence, and time period.

Presented in abstract form as an oral presentation at the 2014 American College of Veterinary Internal Medicine Forum, Nashville, TN, USA.

* Corresponding author.

E-mail address: scansen.2@osu.edu (B.A. Scansen).

¹ Dr. Visser's current address: Department of Medicine & Epidemiology, School of Veterinary Medicine, University of California-Davis, Davis, CA, USA.

Results: All indices showed a significant ($p < 0.0001$) increase and decrease from baseline following pimobendan and atenolol, respectively. Significant differences from baseline were attributed to drug treatment ($p < 0.0001$); whereas, effects of other covariates were not significant. The greatest percent changes, but also highest variability, were observed for S' and strain rate ($p < 0.0001$). Post-atenolol, a significantly greater proportion of dogs exceeded the repeatability coefficient of variation for FAC and S' compared to TAPSE ($p \leq 0.007$).

Conclusions: Echocardiographic indices in healthy dogs tracked expected changes in RV systolic function following pimobendan and atenolol and warrant study in dogs with cardiovascular disease.

© 2015 Elsevier B.V. All rights reserved.

Abbreviations

2D	two-dimensional
CMR	cardiac magnetic resonance
EF	ejection fraction
FAC	fractional area change
RV	right ventricular
RVA _D	right ventricular area at end-diastole
RVA _S	right ventricular area at end-systole
S'	pulsed wave tissue Doppler imaging-derived systolic myocardial velocity of the lateral tricuspid annulus
SD	standard deviation
STE	speckle tracking echocardiography
TAPSE	tricuspid annular plane systolic excursion
TDI	tissue Doppler imaging

Introduction

The clinical assessment of right ventricular (RV) systolic function is underdeveloped and has largely been ignored in dogs. In contrast, the quantitative assessment of RV function in people is useful for clinical decision-making and provides prognostic data for those affected with right heart-specific diseases,¹ as well as left heart-specific diseases including mitral and aortic valve disease^{2–4} and idiopathic dilated cardiomyopathy,^{5–10} often independent of pulmonary hypertension status. Similar diseases affect dogs; therefore, a study investigating the quantitative assessment of canine RV function is warranted.

Echocardiography is the most practical method for assessment of RV structure and function, though is limited by load-dependence, coarse trabeculae, and subdivided anatomy that is less amenable to geometric shape assumptions.¹¹ Despite these challenges, physicians utilize a

number of echocardiographic indices of RV function, each with inherent advantages and disadvantages that have been validated against a gold standard. These indices include M-mode-derived tricuspid annular plane systolic excursion (TAPSE), the 2-dimensional (2D) surrogate of RV ejection fraction (EF) – RV percent fractional area change (FAC), tissue Doppler imaging (TDI)-derived systolic myocardial velocity of the lateral tricuspid annulus (S'), and speckle-tracking echocardiography (STE)-derived systolic longitudinal RV strain and strain rate.^{12–16}

Echocardiographic indices of RV systolic function may be useful for the identification and quantification of RV dysfunction in the dog, but studies attempting to validate these indices are needed. This study evaluated 5 echocardiographic indices of RV systolic function in the conscious healthy dog over 3 contractile states (baseline, increased and decreased function). Specifically, the objective of this study was to determine if TAPSE, FAC, S' , global longitudinal RV free wall STE-derived strain and strain rate could track anticipated changes in RV systolic function following a single oral dose of pimobendan and atenolol in dogs. We hypothesized that the proposed echocardiographic indices can be acquired and used to detect changes in RV systolic function following the administration of pimobendan (expected to increase systolic function) and atenolol (expected to decrease systolic function) in conscious healthy dogs.

Animals, materials and methods

All procedures in this study were approved by the Institutional Animal Care and Use Committee and the Veterinary Medical Center Clinical Research and Teaching Advisory Committee at The Ohio State University. Written consent authorizing

participation of dogs in the study was obtained from all dog owners.

Animals

Eighty privately-owned mature (≥ 8 months) dogs of varying breed and body weight ($n = 40 > 15$ kg; $n = 40 \leq 15$ kg) were enrolled in this study as well as another study determining repeatability and reference intervals for RV systolic function indices.¹⁷ To be enrolled, dogs had to be deemed healthy based on medical history, physical examination, and a thorough screening echocardiogram and were excluded if they 1) had pathologic heart murmur, gallop sound, or (non-sinus) arrhythmia; 2) had history of respiratory disease; 3) were taking medications known to affect the cardiovascular or respiratory system; 4) demonstrated an uncooperative temperament during the screening echocardiogram; 5) were a Boxer dog or English bulldog (due to risk of undetected arrhythmogenic RV cardiomyopathy); and 6) had an abnormality identified on a baseline 2D, M-mode, and Doppler echocardiogram. Due to the high prevalence of canine physiologic tricuspid and pulmonary valve regurgitation,¹⁸ tricuspid or pulmonary valve regurgitation discovered with color Doppler echocardiography was permitted given that it was silent to auscultation and valve morphology was normal.

Study design

This was a prospective, blinded, randomized, crossover study. Immediately following a baseline echocardiographic study, each dog was administered a single oral dose of either pimobendan^c (0.25 mg/kg) or atenolol (1 mg/kg). The order of drug administration was randomized^d with drug administration blinded to the investigators. Three hours post-pill, all dogs underwent a second echocardiographic study to evaluate the effect of the drug on RV systolic function. This time point was selected because in the dog, peak blood concentration of both pimobendan¹⁹ and atenolol²⁰ have been shown to occur within approximately 3 h following oral administration. Within a 3-week time period and following a minimum 72-h washout period, each dog underwent a second baseline and post-drug echocardiographic study using the alternate drug. Thus, each dog underwent four echocardiographic studies – twice for

baseline, once after pimobendan, and once after atenolol.

Echocardiographic examination

Conventional and Doppler echocardiography

All echocardiographic studies were performed by the same trained investigator (L.C.V.) using continuous ECG monitoring and an echocardiographic system^e equipped with 4S (1.5–5.0 MHz), 7S (3.5–8.0 MHz), and 10S (4.4–10 MHz) phased-array transducers matched to the size of the dog. Dogs were manually restrained in right and left lateral recumbency without the use of sedation. Conventional imaging planes²¹ were utilized and all raw data were captured digitally for off-line analysis at a digital workstation.

Echocardiographic indices of right ventricular systolic function

All indices of RV systolic function were acquired from a modified (more cranial) left apical 4-chamber view optimized for the right heart in which the longitudinal dimension of the RV was maximized. At least 10 cardiac cycles of each RV function index were acquired and stored, with the value for each RV function index at each time point determined from the average of 5 representative and not necessarily consecutive cardiac cycles. The heart rate recorded represented the average heart rate of each of the 5 cardiac cycles used to determine the RV function index value. Image quality and resolution of the RV myocardial and endomyocardial borders (including the RV apex region) were continuously assessed and optimized. An attempt was made to record and store data during periods of eupnea.

Measurement of TAPSE consisted of quantifying the maximal longitudinal displacement of the lateral tricuspid valve annulus toward the RV apex and was generated from M-mode recordings with the cursor as parallel as possible to the majority of the RV free wall (Fig. 1). On rare occasion (<10% of recordings) the anatomic M-mode technique²² was activated on stored images when conventional M-mode recordings were suboptimal e.g., inadequate parallel alignment to the RV free wall or an inability to clearly identify the tricuspid annular motion on the M-mode recording. Measurements for TAPSE were made in a leading edge-to-leading edge manner at sweep speeds of at least 66 mm/s. For FAC determination, measurements of RV area

^c Vetmedin, Boehringer Ingelheim Vetmedica, Inc., St. Joseph, MO, USA.

^d <http://www.randomizer.org/>.

^e Vivid 7 Dimension with EchoPAC software package, version BT09, GE Medical Systems, Waukesha, WI, USA.

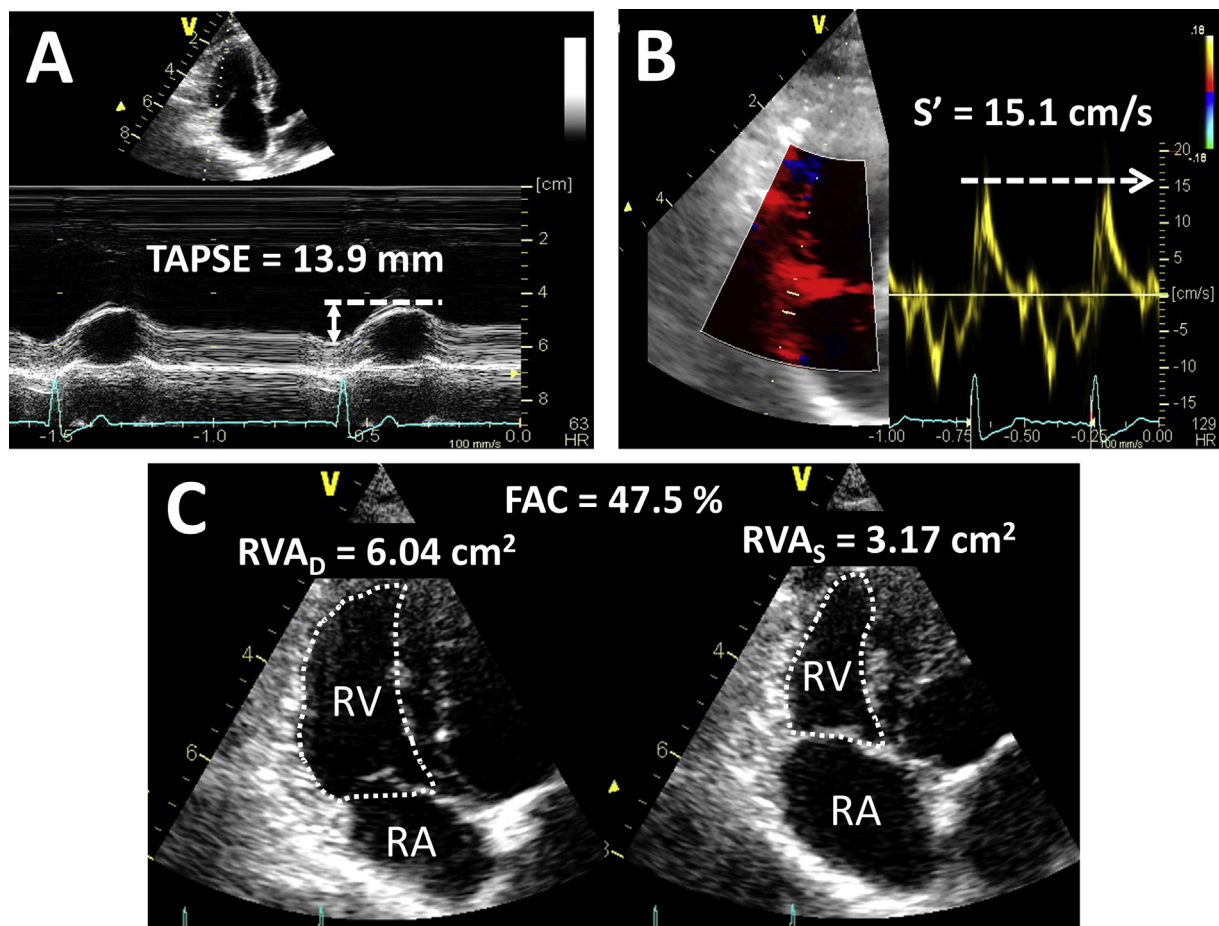


Figure 1 Representative measurements of tricuspid annular plane systolic excursion (TAPSE) (A), pulsed-wave tissue Doppler imaging (TDI)-derived peak systolic longitudinal myocardial motion velocity at the lateral tricuspid annulus (S') (B), and right ventricular (RV) percent fractional area change (FAC) (C). For TAPSE, measurements quantify maximal longitudinal displacement of the lateral tricuspid valve annulus toward the RV apex during systole using M-mode echocardiography. For FAC, measurements of RV area were obtained by tracing the RV endocardial border (dotted lines) at end-diastole (RVA_D) and end-systole (RVA_S). The FAC is calculated using the formula: $FAC = ([RVA_D - RVA_S]/RVA_D) \times 100$. RA, right atrium; RV, right ventricle.

were obtained by tracing the RV endocardial border at end-diastole (RVA_D), defined as the onset of the R wave on the ECG, and end-systole (RVA_S), defined as the smallest chamber dimension immediately prior to tricuspid valve opening (Fig. 1). Right ventricular percent FAC was calculated using the formula: $FAC = ([RVA_D - RVA_S]/RVA_D) \times 100$. Pulsed-wave TDI of longitudinal myocardial motion at the level of the lateral tricuspid annulus was obtained to measure peak systolic myocardial velocity of the lateral tricuspid annulus (S') (Fig. 1). For accurate S' determination, the cursor was aligned as parallel as possible with the majority of the RV free wall, sample volume varied from 1 to 4 mm based on size of dog, and frame rate was maximized (at least 125 frames/

second). Measurements of S' were made at sweep speeds of at least 66 mm/s.

Strain and strain rate measurements were made with proprietary 2D speckle-tracking software.^f As no defined RV STE algorithm was available, the left ventricular 2 chamber algorithm was employed. The optimal frame rate for canine RV STE is currently unknown; therefore, three 2D RV cine loops each were acquired at maximum, at 1 setting less than maximum, and at 2 settings less than the maximum frame rate. Event timing for pulmonary valve opening and closure was timed to the ECG via a continuous wave Doppler recording of pulmonary outflow velocity. Large deviations in heart rate were avoided for event timing, as these measurements were made on cardiac cycles separate from

^f EchoPAC 2D Strain software, Q-Analysis (strain module), version 6.1, GE Medical Systems, Waukesha, WI, USA.

the measured indices. Only RV free wall longitudinal strain and strain rate were studied as longitudinal motion has been recognized to be the major contributor to RV contraction in the dog.²³ The region of interest for STE was defined by manually tracing the RV free wall endocardial border from the level of the tricuspid valve annulus to the RV apex followed by adjustments to incorporate the entire RV free wall myocardial thickness. Individual RV segments were then visually analyzed to assure adequate myocardial tracking by the software and manually adjusted if necessary. Tracking was accepted if both visual inspection and software inspection (green color coding conformation) confirmed it was adequate. If software approval was unobtainable, it was manually overridden only if visual inspection of myocardial tracking was considered adequate during slow motion playback. The frame rate that provided the most accurate tissue tracking based on visual and software inspection was chosen for STE-derived strain and strain rate (generally > 80 frames/second). Strain and strain rate values were generated by the software for each of 3 myocardial segments (basilar, mid, and apical myocardium of the RV free wall) in addition to the global values from the entire RV (considered as a single segment and not a mean of the 3 segments). Only systolic global longitudinal strain and strain rate values of the RV free wall were utilized in this study and were determined as the maximal (most negative) systolic point on the respective global strain or strain rate curve prior to pulmonary valve closure (Fig. 2).

Statistical analysis

All statistical analyses were performed using commercial software.^{g,h} Normality testing for continuous data consisted of visual inspection of probability plots and the D'Agostino–Pearson test.

For each echocardiographic index of RV systolic function following each drug, the Wilcoxon signed-rank test was used to compare the post-drug echocardiogram to its respective same-day baseline.

For each RV function index, a linear mixed-effects regression model was used to compare percent change in RV function from the same-day baseline. The model included a random subject (dog) effect with fixed effects for treatment (pimobendan or atenolol), drug sequence, and time period. Other covariates included for

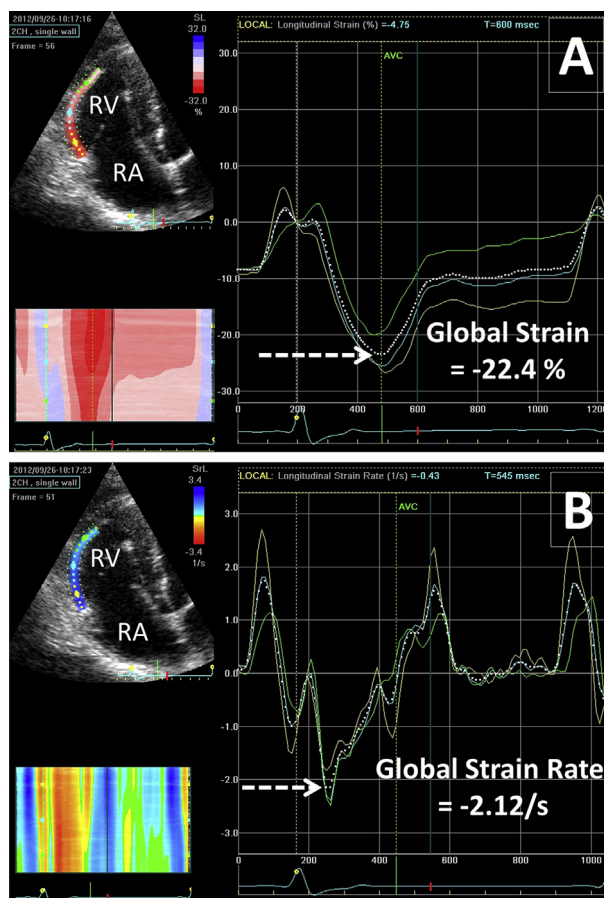


Figure 2 Representative images of the workstation output for right ventricular (RV) free wall longitudinal strain (A) and strain rate (B). A reference 2D image of the right heart can be seen in the upper left, a color map is shown in the lower left to display the change in strain or strain rate over one cardiac cycle, and the remainder of the snapshot includes 3 regional (basilar = yellow, mid = light blue, apical = green) and global (dotted line) strain or strain rate curves over time in relation to the ECG (bottom). Only systolic global longitudinal strain and strain rate of the RV free wall prior to pulmonary valve closure was utilized in this study (arrows). The label “AVC” corresponds to pulmonary valve closure (instead of aortic valve closure [AVC]) determined from a continuous wave Doppler recording of pulmonary outflow timed with the ECG. RA, right atrium; RV, right ventricle.

adjustment in estimation of the treatment effects were heart rate (in bpm), body weight (in kg), gender (male or female), and age (in months). For all linear regression models, assumptions of linearity, homoscedasticity, and normality of the residuals were evaluated by inspection of the standardized residual plots and probability plots.

^g GraphPad Prism, version 5.04, GraphPad Software, Inc., San Diego, CA, USA.

^h SAS, version 9.2, SAS Institute Inc., Cary, NC, USA.

Friedman's test was performed as an additional method to compare percent change of each RV function index to the percent change in RV function from baseline following pimobendan and atenolol. If the test was statistically significant, post-hoc comparisons of the RV function indices consisted of multiple Wilcoxon signed rank tests while adjusting the p -value based on the Holm–Bonferroni (sequentially rejective) method for the number of comparisons.

In order to compare the RV function indices post-pimobendan and post-atenolol, a chi-squared test was performed on the proportion of dogs whose RV function index did or did not exceed the average repeatability coefficient of variation (i.e., the day-to-day variability) specific to each RV function index.¹⁷ A similar analysis was performed on the proportion of dogs whose RV function index was or was not outside the body weight-specific reference interval specific to each RV function index.¹⁷ If the chi-squared test was statistically significant, post-hoc comparison of RV function indices using multiple z-tests for comparing two proportions, while adjusting the p -value based on the Holm–Bonferroni (sequentially rejective) method for the number of comparisons. A value of $p < 0.05$ was considered statistically significant for all comparisons.

Results

Animals

Dogs ($n = 36$ castrated males; $n = 44$ spayed females) in the current study had a mean age of 4.1 ± 2.5 years (min = 0.66, max = 9 years) and a mean body weight of 18 ± 11 kg (min = 3.9, max = 42.3 kg). A variety of mixed breeds ($n = 41$) and purebreds ($n = 5$ Pugs; $n = 4$ Boston Terriers, Labrador Retrievers, Golden Retrievers, and Miniature Schnauzers; $n = 2$ Cavalier King Charles Spaniels, Rat Terriers, Italian Greyhounds, Chihuahuas, Beagles, and German Shepherds; $n = 1$ Border Collie, Wheaten Terrier, Bloodhound, Miniature Pinscher, Greyhound, Pembroke Welsh Corgi, English Setter, Toy Poodle, Pomeranian, and Papillon) made up the study sample.

Indices of RV function following pimobendan and atenolol

Each RV function index could be acquired in all dogs. Baseline average heart rate throughout the echocardiographic evaluation was 107 ± 24 bpm

prior to pimobendan and 102 ± 25 bpm post-pimobendan. Baseline average heart rate prior to atenolol administration was 103 ± 23 bpm and 84 ± 19 bpm post-atenolol. Right ventricular systolic function indices before and after pimobendan and atenolol are summarized in Table 1 and the percent change from respective baseline following each drug is displayed graphically in Figure 3. For each RV function index following each drug, a statistically significant difference (all $p < 0.0001$) was found when each baseline study was compared to its same-day post-drug echocardiogram (Table 1).

A treatment effect, evidenced by a mean percent change in RV systolic function from baseline after pimobendan and atenolol was significantly different for each index (all $p < 0.0001$). None of the other covariates (gender, body weight, age, heart rate, drug sequence, or time period) demonstrated a significant effect on the model for any of the RV function indices.

Comparing the RV function indices as a percent increase from baseline post-pimobendan (Fig. 4), both S' and strain rate showed the largest increase in RV function from baseline and were both significantly (all $p < 0.0001$) greater than the other indices but not from each other. The FAC detected a significantly larger increase in RV function from baseline compared to strain and TAPSE (both $p < 0.0001$). Following atenolol, S' and strain rate demonstrated the largest decline in RV function from baseline, both significantly larger than FAC, strain, and TAPSE (all $p \leq 0.002$) but not significantly different from each other (Fig. 5). The FAC detected a significantly larger decrease in RV function compared to TAPSE ($p < 0.0001$).

The RV function indices detected changes in RV function exceeding the average repeatability coefficient of variation (day-to-day variability) post-pimobendan or atenolol in at least 74% (59 of 80) of the dogs (Table 2). Chi-squared analysis comparing the proportion of dogs for each RV function index whose post-pimobendan value exceeded the repeatability coefficient of variation failed to reach statistical significance ($p = 0.069$). Both FAC and S' had a significantly higher proportion of dogs whose RV function index post-atenolol exceeded the repeatability coefficient of variation compared to TAPSE (both $p \leq 0.007$).

The proportion of dogs whose RV function index post-pimobendan and post-atenolol was outside their respective body weight-specific reference interval¹⁷ is reported in Table 3. After pimobendan, FAC showed a significantly higher proportion of dogs above the reference interval compared to TAPSE and strain (both $p \leq 0.005$).

Table 1 Indices of right ventricular systolic function at baseline and 3-h post-pimobendan and post-atenolol in 80 conscious healthy dogs. Data presented as median (interquartile range) as the majority failed normality testing except where indicated.

RV function index	Pimobendan		Atenolol	
	Baseline	3-h post ^b	Baseline	3-h post ^c
TAPSE (mm)	13.12 (11.25 to 15.17)	14.65 (12.72 to 16.89)	13.48 (11.44 to 15.71)	11.79 (9.94 to 13.45)
FAC (%)	47.11 (41.42 to 50.94)	55.46 (50.77 to 61.85)	46.52 (41.32 to 51.33)	36.58 (33.61 to 40.45)
S' (cm/s)	13.13 (10.44 to 15.22)	17.81 (13.38 to 20.55)	13.24 (10.35 to 15.85)	9.09 (7.18 to 11.85)
Strain × -1 (%)	28.68 (25.60 to 30.34)	31.56 (29.78 to 35.00)	29.07 (26.15 to 30.85)	24.18 (21.38 to 26.68)
Strain rate × -1 (s ⁻¹)	3.18 (2.60 to 3.65)	4.11 (3.27 to 4.88)	3.30 (2.59 to 3.85)	2.40 (1.97 to 2.76)
% change ^d				
		13.18% ^a (5.75 to 18.62)		-12.05% ^a (-4.41 to -18.42)
		18.44% (10.49 to 29.86)		-18.85% ^a (-12.63 to -23.37)
		31.66% ^a (18.21 to 47.08)		-24.11% ^a (-16.91 to -36.71)
		12.55% ^a (7.96 to 19.58)		-15.19% ^a (-9.73 to -22.13)
		27.52% ^a (15.61 to 47.98)		-26.03% (-15.26 to -32.99)

RV, right ventricular; TAPSE, tricuspid annular plane systolic excursion; FAC, fractional area change; S', pulsed wave tissue Doppler-derived lateral tricuspid annular longitudinal peak systolic velocity.

^a Data were normally distributed.

^b Each RV function index demonstrated a significant (all $p < 0.0001$) increase compared to its respective baseline.

^c Each RV function index demonstrated a significant (all $p < 0.0001$) decrease compared to its respective baseline.

^d For each RV function index, percent (%) change in RV systolic function post-drug had a significant (all $p < 0.0001$) effect based on the mixed-model analysis.

Following atenolol, FAC had a significantly higher proportion of dogs below the reference interval compared to TAPSE and S' (both $p = 0.009$).

Discussion

The results presented confirmed the hypothesis that the studied echocardiographic indices can be acquired in conscious healthy dogs and can track changes in RV systolic function following the oral administration of pimobendan and atenolol at clinically relevant doses. Multivariate analysis indicated that the percent changes in RV systolic function post-drug were not significantly affected by heart rate, body weight, gender, age, drug sequence, or examination time, but did show significant changes after drug administration. All of the RV function indices were able to detect changes beyond the day-to-day variability in the majority of dogs; these indices may therefore detect clinically relevant changes in RV systolic function.

Studies designed to validate echocardiographic indices of cardiac function in veterinary medicine have traditionally compared the studied index to an invasive gold standard and provide valuable information. However, such studies commonly involve a small number of healthy dogs of similar body type or breed (e.g., purpose-bred research beagles or hounds) that are subject to the negative inotropic effects and risks of general anesthesia, thus limiting clinical extrapolation of the results. Application of such data to the general canine population is also limited by homogeneity in the study group because the clinical canine population varies widely by age, breed, and body weight. The current study design did not require general anesthesia and enrolled a relatively large, diverse sample consisting of dogs of various size, breed, and age. Therefore, we consider our approach clinically relevant and a noninvasive acceptable alternative as a proof of concept, despite the lack of an invasive gold standard.

Tissue Doppler imaging (TDI)-derived systolic myocardial velocity of the lateral tricuspid annulus (S') represents a region-specific index of RV longitudinal systolic function. Advantages of pulsed wave TDI-derived S' include that it is quick, easy-to-perform, and less geometry-dependent than other echocardiographic indices. It is limited by its angle-dependence, region specificity, and, together with TAPSE, it has been shown to be less accurate in the setting of severe tricuspid regurgitation in people.²⁴ Color TDI-derived RV myocardial velocities have been shown to be

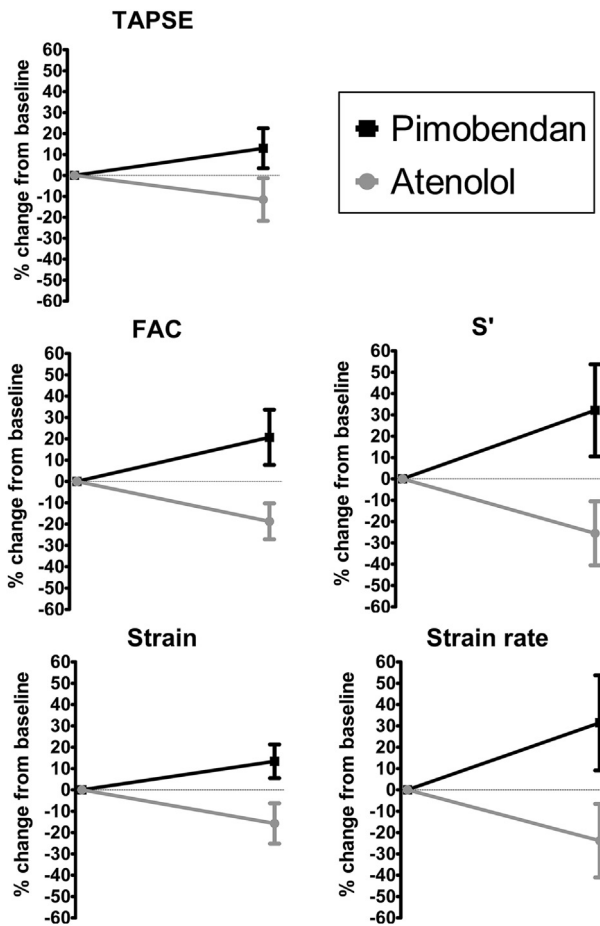


Figure 3 Mean \pm SD percent (%) change in right ventricular (RV) systolic function from baseline post-pimobendan (black line) and post-atenolol (gray line) as quantified by tricuspid annular plane systolic excursion (TAPSE), RV percent fractional area change (FAC), pulsed wave tissue Doppler-derived lateral tricuspid annular longitudinal peak systolic velocity (S'), RV free wall global longitudinal strain ("Strain") and RV free wall global longitudinal strain rate ("Strain rate"). Percent change in RV systolic function from baseline post-atenolol was significantly different compared to post-pimobendan for each RV systolic function index (all $p < 0.0001$). Note both the degree of change (% change from baseline) and the variation of the change (SD error bars) following pimobendan and atenolol for each RV systolic function index.

repeatable and reproducible,²⁵ and vary with the severity of pulmonary hypertension in the dog.²⁶ Color TDI-derived RV systolic velocities may also be of value in the early prediction of dilated cardiomyopathy in the dog.²⁷ With the exception of S' ,²⁸ few validation (proof-of-concept) studies on the echocardiographic assessment of RV systolic function have been performed in the dog. Hori et al.²⁸ demonstrated that pulsed wave TDI-derived S' strongly correlated ($r = 0.93$) with one

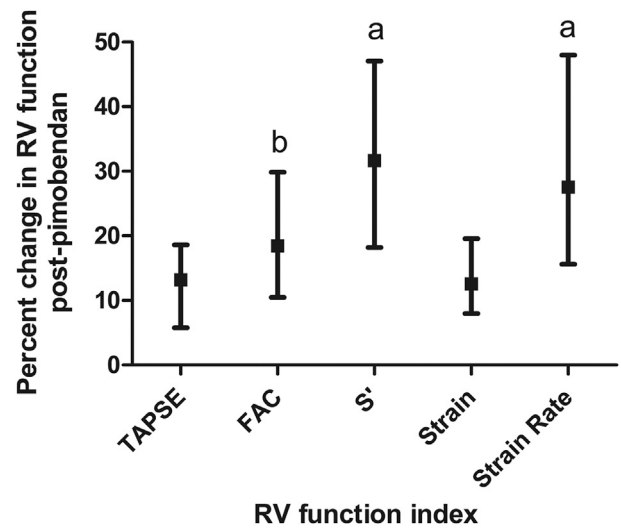


Figure 4 Median \pm interquartile range for percent change (increase) in RV function as quantified by TAPSE, FAC, S' , Strain, and Strain Rate post-pimobendan. A Friedman's test showed the RV function indices were statistically different ($p < 0.0001$). ^aPercent increase in RV function from baseline was significantly greater than FAC, strain, and TAPSE (all $p < 0.0001$). ^bPercent increase in RV function from baseline was significantly greater than strain and TAPSE (both $p < 0.0001$). See Figure 3 for key.

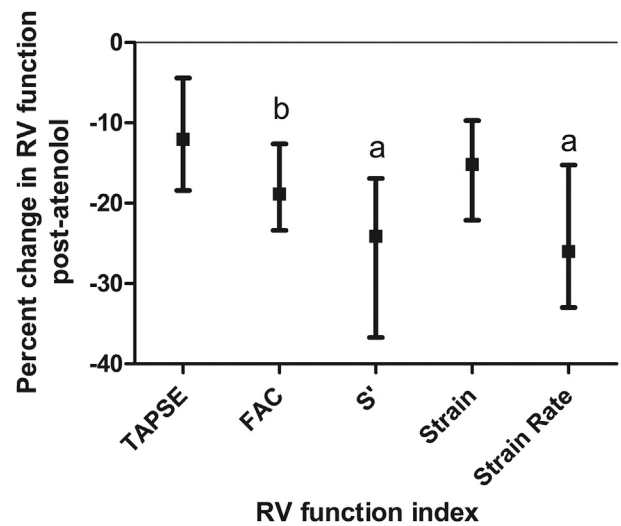


Figure 5 Median \pm interquartile range for percent change (decrease) in RV function as quantified by TAPSE, FAC, S' , Strain, and Strain rate post-atenolol. A Friedman's test showed the RV function indices were statistically different ($p < 0.0001$). ^aPercent decrease in RV function from baseline was significantly greater than FAC, strain, and TAPSE (all $p \leq 0.002$). ^bPercent decrease in RV function from baseline was significantly greater than TAPSE ($p < 0.0001$). See Figure 3 for the key.

Table 2 Proportion of dogs whose percent change in right ventricular function post-pimobendan and post-atenolol exceeded the repeatability coefficient of variation.

RV function index	CV (%) ^a	Post-pimobendan ^b	Post-atenolol
TAPSE	4.7	64/80	59/80
FAC	4.3	75/80	76/80 ^c
S'	7.8	68/80	73/80 ^c
Strain	4.0	73/80	72/80
Strain Rate	8.5	71/80	68/80

CV, coefficient of variation. See Table 1 for reminder of the key.

^a Repeatability CV values reported from 80 healthy dogs.¹⁷

^b Chi-squared analysis comparing the RV function indices post-pimobendan did not reach statistical significance ($p = 0.069$).

^c When comparing the RV function indices post-atenolol, FAC and S' were significantly different from TAPSE (both $p \leq 0.007$).

variable of RV contractility (+dP/dtmax) over a range of inotropic states in seven anesthetized healthy beagles. Interestingly, in that study,²⁸ S' was not significantly decreased compared to baseline following the intravenous administration of the negative inotrope esmolol (low or high dose), which is in contrast to the current study where S' was significantly decreased from baseline following oral administration of atenolol. The inability of Hori et al.²⁸ to measure a difference may be explained by a baseline depression of RV systolic function secondary to general anesthesia in their dogs prior to the administration of the esmolol, in addition to a lack of statistical power given the small number of dogs.²⁸ Pulsed wave TDI-derived S' has also been shown to correlate well with radionuclide ventriculography in people with a variety of right heart diseases,²⁹ and with cardiac magnetic resonance (CMR)-derived RV EF in people with congenital heart disease³⁰ and arrhythmogenic RV cardiomyopathy.³¹

Similar to S', TAPSE is one of the simplest methods to assess RV longitudinal systolic function. Measurement of TAPSE involves determination of the apical displacement of the tricuspid valve annulus during systole from an M-mode recording. It is, however, another angle-

dependent, region-specific index that may be adversely affected by translational motion. A recent study³² revealed that TAPSE is decreased in dogs with varying severities of pulmonary hypertension and below the reference interval in most dogs with severe pulmonary hypertension. TAPSE has been validated in healthy people³³ and has been shown to correlate well with radionuclide-³⁴ and CMR-derived RV EF³⁵ in people with RV dysfunction.

Right ventricular FAC represents a 2D surrogate of RV EF from an apical imaging plane. Right ventricular FAC correlates best to CMR-derived RV EF as compared to other 2D echocardiographic indices of RV systolic function in people, performing better than TAPSE.³⁶ Unlike the other RV function indices studied, FAC is not solely an index of RV longitudinal function; instead incorporating an additional plane to assess RV function. Despite its ease of measurement and less acquisition angle-dependence, it may be less favorable in patients with poor image quality because of the necessity for accurate RV endocardial border detection.

Speckle-tracking echocardiography-derived strain and strain rate are relatively new indices of myocardial function and are based on

Table 3 Proportion of dogs whose right ventricular function index post-pimobendan and post-atenolol were outside their respective body weight-specific reference interval.

RV function index	Post-pimobendan (above the RI)	Post-atenolol (below the RI)
TAPSE	8/80	15/80
FAC	27/80 ^a	31/80 ^b
S'	20/80	15/80
Strain	11/80	26/80
Strain rate	20/80	26/80

RI, reference interval. See Table 1 for reminder of the key.

^a When comparing the RV function indices post-pimobendan, FAC was significantly different from TAPSE and strain (both $p \leq 0.005$).

^b When comparing the RV function indices post-atenolol, FAC was significantly different from TAPSE and S' (both $p = 0.009$).

quantifying tissue deformation (strain) or tissue deformation over time (strain rate) globally or in a region-specific manner. Despite their post-processing and time-consuming nature, a large advantage of STE-derived indices is their acquisition angle-independence, which is well suited for the RV given its complex geometry. Right ventricular free wall STE-derived longitudinal strain and strain rate were recently demonstrated to correlate well with CMR-derived RV EF, mean pulmonary artery pressure, and pulmonary vascular resistance in people affected with pulmonary hypertension.³⁷

The current study was designed to determine if 5 echocardiographic indices of RV systolic function could detect anticipated changes in systolic function induced by pimobendan and atenolol in healthy dogs. It was not necessarily designed to compare the 5 RV systolic function indices to each other, as none are a recognized gold standard. Several post-hoc comparisons attempting to determine differences in the RV function indices' ability to track changes in systolic function were performed. The comparison of the indices involving the proportion of dogs whose RV function index surpassed day-to-day variability (repeatability coefficient of variation) post-drug may be the most relevant to clinical practice, as most diseases that affect the RV are likely to cause a decrease in function. Based on our results, FAC and S' may be better suited than TAPSE to detect decreases in RV function beyond day-to-day variability, but studies designed to specifically test this hypothesis in diseased dogs would be required. It is important to consider that the RV function index with the greatest percent change may not be superior to the others at tracking systolic function. The RV function indices S' and strain rate showed the largest magnitude of change with alteration of systolic function in this study, but the variability of these indices are greater than the other indices and may limit their utility. Ultimately, it is our hope that the current study and the post-hoc comparisons performed stimulate further studies assessing and comparing RV function indices in dogs affected with various cardiopulmonary diseases.

This study has several limitations. There was no gold standard of RV systolic function measured for comparison with the echocardiographic indices. However, as indicated previously, current gold standards for evaluation of cardiac function require general anesthesia thereby limiting their clinical use. Importantly, the requirement for

general anesthesia is an inherent disadvantage when evaluating cardiac function. Anesthetics depress systolic function and transthoracic echocardiography, as routinely acquired in dogs, is not performed under general anesthesia. Although lacking a gold standard, the reduction in heart rate seen in the atenolol arm of the study can be viewed as a global measure of drug effect as would be expected from beta-blockade. Additionally, post-hoc analysis of concurrent echocardiographic studies taken of the left ventricle supported the expected global effect of pimobendan with an increase in systolic function indices post-drug. This study also enrolled healthy dogs and evaluated RV function under a medically-altered change in systolic function; it is unknown if the echocardiographic indices of RV function studied track changes in RV function related to naturally-occurring disease in the same way, although the same directional changes observed would be anticipated. The effect of pimobendan on pulmonary vascular resistance also must be considered as afterload reduction, in addition to increased inotropy, may account for some of the measured change. We cannot separate the unique effects of an inodilator on both contractility and afterload without invasive measurement. Consequently, some of the measured change seen with pimobendan may relate to alterations in pulmonary vascular resistance; however, the increased inotropic effect of pimobendan is well documented in the dog¹⁹ and this, coupled with the effect measured by atenolol, argues that these indices can be used as a surrogate to track changes in RV systolic function. Studies show that RV function is partially determined by left ventricular function³⁸; as such, we cannot be certain how much of an effect pharmacologic alteration of left ventricular function had on these measures of RV function. An additional limitation of the current study is the lack of longitudinal follow-up for the dogs enrolled in this study. Without longitudinal follow-up, sub-clinical cardiac disease that could affect RV function may be missed, which could impact the response of RV function to the drugs administered. Also, these indices were evaluated over a wide range of body weight; the performance of these indices in dogs outside the body weights encountered in the current study (<3.9 kg and >42.3 kg) cannot be ascertained. Last, the drugs studied cause observable effects on heart rate and cardiac motion, which are visible during echocardiographic evaluation and may have impaired complete blinding.

Conclusions

This study showed that 5 echocardiographic indices of RV systolic function, each with their own inherent advantages and disadvantages, were consistently able to track changes in RV systolic function following induced positive and negative variation of systolic function in conscious healthy dogs. Further studies are warranted to determine the value of these indices of RV function in dogs with spontaneous cardiovascular or respiratory disease.

Conflicts of interest

The authors declare no conflicts of interest.

Acknowledgments

This study was supported by the American Kennel Club Canine Health Foundation Clinician-Scientist Fellowship Program (L.C.V.). The authors would like to thank Tammy Muse, Patti Mueller, and Drs. Kay Drake and Kyla Morgan for technical assistance, and the dog owners of The Ohio State University College of Veterinary Medicine community for volunteering their dogs.

References

- Haddad F, Doyle R, Murphy DJ, Hunt SA. Right ventricular function in cardiovascular disease, part II: pathophysiology, clinical importance, and management of right ventricular failure. *Circulation* 2008;117:1717–1731.
- Le Tourneau T, Deswarte G, Lamblin N, Foucher-Hossein C, Fayad G, Richardson M, Polge AS, Vannesson C, Topilsky Y, Juthier F, Trochu JN, Enriquez-Sarano M, Bauters C. Right ventricular systolic function in organic mitral regurgitation: impact of biventricular impairment. *Circulation* 2013;127:1597–1608.
- Hochreiter C, Niles N, Devereux RB, Kligfield P, Borer JS. Mitral regurgitation: relationship of noninvasive descriptors of right and left ventricular performance to clinical and hemodynamic findings and to prognosis in medically and surgically treated patients. *Circulation* 1986;73:900–912.
- Nagel E, Stuber M, Hess OM. Importance of the right ventricle in valvular heart disease. *Eur Heart J* 1996;17:829–836.
- Meluzin J, Spinarova L, Hude P, Krejci J, Kincl V, Panovsky R, Dusek L. Prognostic importance of various echocardiographic right ventricular functional parameters in patients with symptomatic heart failure. *J Am Soc Echocardiogr* 2005;18:435–444.
- Ghio S, Gavazzi A, Campana C, Inserra C, Klersy C, Sebastiani R, Arbustini E, Recusani F, Tavazzi L. Independent and additive prognostic value of right ventricular systolic function and pulmonary artery pressure in patients with chronic heart failure. *J Am Coll Cardiol* 2001;37:183–188.
- Di Salvo TG, Mathier M, Semigran MJ, Dec GW. Preserved right ventricular ejection fraction predicts exercise capacity and survival in advanced heart failure. *J Am Coll Cardiol* 1995;25:1143–1153.
- La Vecchia L, Bedogni F, Castellani A, Martini M, Paccanaro M, Sartori M, Bozzola L, Bevilacqua P, Vincenzi M. Assessment of right ventricular function and interstitial fibrosis in idiopathic dilated cardiomyopathy: hemodynamic correlates and prognostic value. *G Ital Cardiol* 1998;28:513–523.
- Juilliere Y, Barbier G, Feldmann L, Grentzinger A, Danchin N, Cherrier F. Additional predictive value of both left and right ventricular ejection fractions on long-term survival in idiopathic dilated cardiomyopathy. *Eur Heart J* 1997;18:276–280.
- de Groote P, Millaire A, Foucher-Hossein C, Nogue O, Marchandise X, Ducloux G, Lablanche JM. Right ventricular ejection fraction is an independent predictor of survival in patients with moderate heart failure. *J Am Coll Cardiol* 1998;32:948–954.
- Haddad F, Hunt SA, Rosenthal DN, Murphy DJ. Right ventricular function in cardiovascular disease, part I: anatomy, physiology, aging, and functional assessment of the right ventricle. *Circulation* 2008;117:1436–1448.
- Horton KD, Meece RW, Hill JC. Assessment of the right ventricle by echocardiography: a primer for cardiac sonographers. *J Am Soc Echocardiogr* 2009;22:776–792.
- Mertens LL, Friedberg MK. Imaging the right ventricle—current state of the art. *Nat Rev Cardiol* 2010;7:551–563.
- Jurcut R, Giusca S, La Gerche A, Vasile S, Ginghina C, Voigt JU. The echocardiographic assessment of the right ventricle: what to do in 2010? *Eur J Echocardiogr* 2010;11:81–96.
- Rudski LG, Lai WW, Afilalo J, Hua L, Handschumacher MD, Chandrasekaran K, Solomon SD, Louie EK, Schiller NB. Guidelines for the echocardiographic assessment of the right heart in adults: a report from the American Society of Echocardiography endorsed by the European Association of Echocardiography, a registered branch of the European Society of Cardiology, and the Canadian Society of Echocardiography. *J Am Soc Echocardiogr* 2010;23:685–713.
- Sheehan F, Redington A. The right ventricle: anatomy, physiology and clinical imaging. *Heart* 2008;94:1510–1515.
- Visser LC, Scansen BA, Schober KE, Bonagura JD. Echocardiographic assessment of right ventricular systolic function in conscious healthy dogs: repeatability and reference intervals. *J Vet Cardiol* 2015;17:83–96.
- Bonagura JD, Miller MW. Doppler echocardiography. II. Color Doppler imaging. *Vet Clin North Am Small Anim Pract* 1998;28:1361–1389.
- Boyle KL, Leech E. A review of the pharmacology and clinical uses of pimobendan. *J Vet Emerg Crit Care* 2012;22:398–408.
- McAinch J, Holmes BF. Pharmacokinetic studies with atenolol in the dog. *Biopharm Drug Dispos* 1983;4:249–261.
- Thomas WP, Gaber CE, Jacobs GJ, Kaplan PM, Lombard CW, Moise NS, Moses BL. Recommendations for standards in transthoracic two-dimensional echocardiography in the dog and cat. Echocardiography Committee of the Specialty of Cardiology, American College of Veterinary Internal Medicine. *J Vet Intern Med* 1993;7:247–252.
- Oyama MA, Sisson DD. Assessment of cardiac chamber size using anatomic M-mode. *Vet Radiol Ultrasound* 2005;46:331–336.

23. Rushmer RF, Crystal DK, Wagner C. The functional anatomy of ventricular contraction. *Circ Res* 1953;1:162–170.
24. Hsiao SH, Lin SK, Wang WC, Yang SH, Gin PL, Liu CP. Severe tricuspid regurgitation shows significant impact in the relationship among peak systolic tricuspid annular velocity, tricuspid annular plane systolic excursion, and right ventricular ejection fraction. *J Am Soc Echocardiogr* 2006;19:902–910.
25. Chetboul V, Sampedrano CC, Gouni V, Concordet D, Lamour T, Ginesta J, Nicolle AP, Pouchelon JL, Lefebvre HP. Quantitative assessment of regional right ventricular myocardial velocities in awake dogs by Doppler tissue imaging: repeatability, reproducibility, effect of body weight and breed, and comparison with left ventricular myocardial velocities. *J Vet Intern Med* 2005;19:837–844.
26. Serres F, Chetboul V, Gouni V, Tissier R, Sampedrano CC, Pouchelon JL. Diagnostic value of echo-Doppler and tissue Doppler imaging in dogs with pulmonary arterial hypertension. *J Vet Intern Med* 2007;21:1280–1289.
27. Chetboul V, Gouni V, Sampedrano CC, Tissier R, Serres F, Pouchelon JL. Assessment of regional systolic and diastolic myocardial function using tissue Doppler and strain imaging in dogs with dilated cardiomyopathy. *J Vet Intern Med* 2007;21:719–730.
28. Hori Y, Kano T, Hoshi F, Higuchi S. Relationship between tissue Doppler-derived RV systolic function and invasive hemodynamic measurements. *Am J Physiol Heart Circ Physiol* 2007;293:H120–H125.
29. Meluzin J, Spinarova L, Bakala J, Toman J, Krejci J, Hude P, Kara T, Soucek M. Pulsed Doppler tissue imaging of the velocity of tricuspid annular systolic motion; a new, rapid, and non-invasive method of evaluating right ventricular systolic function. *Eur Heart J* 2001;22:340–348.
30. Lytrivi ID, Lai WW, Ko HH, Nielsen JC, Parness IA, Srivastava S. Color Doppler tissue imaging for evaluation of right ventricular systolic function in patients with congenital heart disease. *J Am Soc Echocardiogr* 2005;18:1099–1104.
31. Wang J, Prakasa K, Bomma C, Tandri H, Dalal D, James C, Tichnell C, Corretti M, Bluemke D, Calkins H, Abraham TP. Comparison of novel echocardiographic parameters of right ventricular function with ejection fraction by cardiac magnetic resonance. *J Am Soc Echocardiogr* 2007;20:1058–1064.
32. Pariaut R, Saelinger C, Strickland KN, Beaufriere H, Reynolds CA, Vila J. Tricuspid annular plane systolic excursion (TAPSE) in dogs: reference values and impact of pulmonary hypertension. *J Vet Intern Med* 2012;26:1148–1154.
33. Kaul S, Tei C, Hopkins JM, Shah PM. Assessment of right ventricular function using two-dimensional echocardiography. *Am Heart J* 1984;107:526–531.
34. Ueti OM, Camargo EE, Ueti Ade A, de Lima-Filho EC, Nogueira EA. Assessment of right ventricular function with Doppler echocardiographic indices derived from tricuspid annular motion: comparison with radionuclide angiography. *Heart* 2002;88:244–248.
35. Ahmad H, Mor-Avi V, Lang RM, Nesser HJ, Weinert L, Tsang W, Steringer-Mascherbauer R, Niel J, Salgo IS, Sugeng L. Assessment of right ventricular function using echocardiographic speckle tracking of the tricuspid annular motion: comparison with cardiac magnetic resonance. *Echocardiography* 2012;29:19–24.
36. Anavekar NS, Gerson D, Skali H, Kwong RY, Yucel EK, Solomon SD. Two-dimensional assessment of right ventricular function: an echocardiographic-MRI correlative study. *Echocardiography* 2007;24:452–456.
37. Fukuda Y, Tanaka H, Sugiyama D, Ryo K, Onishi T, Fukuya H, Nogami M, Ohno Y, Emoto N, Kawai H, Hirata K. Utility of right ventricular free wall speckle-tracking strain for evaluation of right ventricular performance in patients with pulmonary hypertension. *J Am Soc Echocardiogr* 2011;24:1101–1108.
38. Friedberg MK, Redington AN. Right versus left ventricular failure: differences, similarities, and interactions. *Circulation* 2014;129:1033–1044.

Available online at www.sciencedirect.com

ScienceDirect